

Communication

Generation of Phosphonium Sites on Sulfated Zirconium Oxide: Relationship to Brønsted Acid Strength of Surface –OH Sites

Jessica Rodriguez, Damien B. Culver, and Matthew P. Conley

J. Am. Chem. Soc., **Just Accepted Manuscript** • DOI: 10.1021/jacs.8b13204 • Publication Date (Web): 09 Jan 2019

Downloaded from <http://pubs.acs.org> on January 10, 2019

Just Accepted

“Just Accepted” manuscripts have been peer-reviewed and accepted for publication. They are posted online prior to technical editing, formatting for publication and author proofing. The American Chemical Society provides “Just Accepted” as a service to the research community to expedite the dissemination of scientific material as soon as possible after acceptance. “Just Accepted” manuscripts appear in full in PDF format accompanied by an HTML abstract. “Just Accepted” manuscripts have been fully peer reviewed, but should not be considered the official version of record. They are citable by the Digital Object Identifier (DOI®). “Just Accepted” is an optional service offered to authors. Therefore, the “Just Accepted” Web site may not include all articles that will be published in the journal. After a manuscript is technically edited and formatted, it will be removed from the “Just Accepted” Web site and published as an ASAP article. Note that technical editing may introduce minor changes to the manuscript text and/or graphics which could affect content, and all legal disclaimers and ethical guidelines that apply to the journal pertain. ACS cannot be held responsible for errors or consequences arising from the use of information contained in these “Just Accepted” manuscripts.

Generation of Phosphonium Sites on Sulfated Zirconium Oxide: Relationship to Brønsted Acid Strength of Surface –OH Sites

Jessica Rodriguez, Damien B. Culver, and Matthew P. Conley*

Department of Chemistry, University of California, Riverside, California 92521, United States

Supporting Information Placeholder

ABSTRACT: The reaction of $(^t\text{Bu})_2\text{ArP}$ (**1a** – **1h**), where the *para* position of the Ar group contains electron donating or electron withdrawing groups, with sulfated zirconium oxide partially dehydroxylated at 300 °C (SZO_{300}) forms $[(^t\text{Bu})_2\text{ArPH}][\text{SZO}_{300}]$ (**2a** – **2h**). The equilibrium binding constants of **1a** – **1h** to SZO_{300} is related to the $\text{p}K_a$ of $[(^t\text{Bu})_2\text{ArPH}]$; R_3P that form less acidic phosphoniums (high $\text{p}K_a$ values) bind stronger to SZO_{300} than R_3P that form more acidic phosphoniums (low $\text{p}K_a$ values). These studies show that Brønsted acid sites on the surface of SZO_{300} are not superacidic.

The control of active site structures in heterogeneous catalysts is important to realize the long standing goal of more selective and reactive solid catalysts.¹ A common method to control the structures of these sites is to support an organometallic complex onto a partially dehydroxylated high surface area oxide to form M–O_x sites (**A**, Figure 1, O_x = surface oxygen) or electrostatic ion-pairs $[\text{M}][\text{O}_x^-]$ (**B**, Figure 1).^{1c,1d} Determining the factors that promote formation of **A**, **B**, or mixtures of these two extremes is fundamentally and practically significant. For example, the reaction of partially dehydroxylated SiO_2 with Cp_2ZrMe_2 forms $\text{Cp}_2\text{Zr}(\text{Me})(\text{OSi}\equiv)$, a type **A** surface species, and is inactive in the polymerization of ethylene.² However, supporting Cp_2ZrMe_2 on partially dehydroxylated sulfated oxides (**SO**) forms $[\text{Cp}_2\text{ZrMe}][\text{SO}]$, a type **B** surface species, that is very active in ethylene polymerization.³ The reaction of organometallic complexes with **SO** usually forms type **B** surface species that are also active in hydrogenation of arenes⁴ and activation of C–H bonds.⁵ Sulfated zirconium oxide (**SZO**) also supports the formation of strong Lewis acid $[\text{iPr}_3\text{Si}][\text{SZO}]$ sites that initiate C–F bond activation reactions.⁶

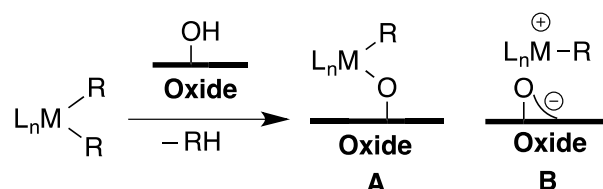
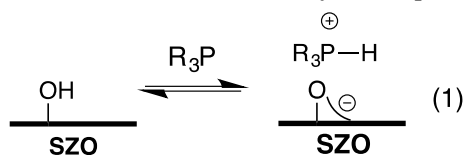


Figure 1. Chemisorption of organometallic complexes onto oxides to form **A** or **B**.

Brønsted acidity of the –OH sites on oxides is often presumed to affect the formation of **A** or **B**. The example reactions of Cp_2ZrMe_2 with oxides are illustrative of this argument. Neutral oxides containing weak Brønsted –OH sites (e.g. SiO_2) tend to form **A**, and oxides containing stronger Brønsted –OH sites (e.g. **SO**) tend to form **B**.

The Brønsted acidity of the –OH sites on **SO** are the subject of a long-standing debate. Initial reports showed that sulfated zirconium oxide (**SZO**) catalyzed the isomerization of n-butane to isobutane at lower temperatures than neat H_2SO_4 .⁷ This result suggests that the Brønsted sites on **SZO** are stronger than neat H_2SO_4 , which would place **SZO** across the threshold of superacidity (Hammett acidity parameter; $H_0 \leq -12.0$).⁸ This observation was supported by adsorption of aromatic colorimetric superacid indicators onto **SZO** showing that $H_0 \leq -16.04$,^{7b} suggesting that the –OH sites on **SZO** are about four orders of magnitude more acidic than H_2SO_4 ($H_0 = -12.0$). However, butane isomerization catalyzed by **SZO** occurs only in the presence of olefin impurities in the reaction feed.⁹ In addition, isothermal calorimetry showed that **SZO** binds pyridine weaker than zeolites.¹⁰ Solid-state NMR studies of **SZO** after adsorption of probe molecules showed that, in addition to Brønsted sites, the **SZO** surface contains Lewis sites,¹¹ and pyrosulfates that are implicated in oxidative reaction pathways.^{5a} Indeed, pyrosulfate sites were suggested to be active in reactions of **SZO** with C–H bonds,¹² and are also implicated in the reaction of organometallic Ir-complexes with **SZO**.^{5a}

This discussion shows some of the complexities in studying the Brønsted acidity of **SZO**. The situation is complicated by the nature of H_0 , which is a property of solution acids. **SZO** is a solid. Among the available methods to assess the Brønsted acidity of solids are temperature programmed desorption of NH_3 ,¹³ measurement ν_{NH} stretches of ammonium salts by FTIR,¹⁴ and changes in chemical shift of adsorbed probe molecules by NMR spectroscopy.¹⁵ This paper describes the reaction of **SZO** with R_3P to form $[\text{R}_3\text{PH}][\text{SZO}]$ (eq 1). The $^{31}\text{P}\{^1\text{H}\}$ NMR chemical shifts of R_3P and $[\text{R}_3\text{PH}]$ are clearly distinguishable and the acidity of $[\text{R}_3\text{PH}]$ spans ~ 15 $\text{p}K_a$ units in MeCN.¹⁶ These properties allow rapid assignment of $[\text{R}_3\text{PH}][\text{SZO}]$ and provide an understanding of how $\text{p}K_a$ of $[\text{R}_3\text{PH}]$ affects the formation of $[\text{R}_3\text{PH}][\text{SZO}]$. These studies show that the Brønsted sites on **SZO** are certainly not superacidic.



SZO was prepared by suspending precipitated zirconium oxide in dilute aqueous H_2SO_4 , followed by calcination at 600 °C. This temperature was chosen because calcination at 600 °C produces **SZO** containing the strongest Brønsted acid sites based on colorimetric titrations. After cooling to room temperature under air, **SZO** was partially dehydroxylated under high vacuum (10^{-6} mbar) at 300 °C to form **SZO**₃₀₀.^{3c}

The reaction of **SZO**₃₀₀ with excess gas phase Me_3P forms $[\text{Me}_3\text{PH}][\text{SZO}_{300}]$ as the major product. The $^{31}\text{P}\{^1\text{H}\}$ Magic Angle Spinning (MAS) spectrum of $[\text{Me}_3\text{PH}][\text{SZO}_{300}]$ contains a major signal at -4 ppm, which is characteristic of $[\text{Me}_3\text{PH}]$ and a minor peak at -33 ppm, assigned to small amounts of Me_3P bound to Lewis sites (Figure S1). This result is important because several previous studies showed that **SZO** reacts with gas phase Me_3P to form mixtures of $\text{O}=\text{PMe}_3$, $[\text{Me}_3\text{PH}]$, and $[\text{Me}_4\text{P}]$.¹¹ Indeed, the reaction of PMe_3 with **SZO** dehydroxylated at 500 °C results in formation of significant amounts of $[\text{Me}_4\text{P}]$ byproducts (Figure S1). The formation of $[\text{Me}_3\text{PH}]$ as the major surface species indicates that **SZO**₃₀₀ does not contain significant quantities of Lewis sites or pyrosulfates that are implicated in the formation of $\text{O}=\text{PMe}_3$ or $[\text{Me}_4\text{P}]$ byproducts.

Reacting bulkier $^t\text{Bu}_3\text{P}$ with **SZO**₃₀₀ (1 equiv/ OH) in Et_2O slurry results in the formation of $[\text{tBu}_3\text{PH}][\text{SZO}_{300}]$, Figure 2a. The FTIR of

$[\text{tBu}_3\text{PH}][\text{SZO}_{300}]$ contains a $\nu_{\text{P-H}}$ at 2441 cm^{-1} (Figure 2b), and the $^{31}\text{P}\{^1\text{H}\}$ MAS NMR spectrum contains a signal at 52 ppm (Figure 2c). ^{31}P NMR signals for other phosphorus species are not observed, consistent with the sole formation of a phosphonium under these conditions. These results indicate that bulky strong donor R_3P are selective probes for Brønsted sites on **SZO**₃₀₀. The clean reactivity of **SZO**₃₀₀ with $^t\text{Bu}_3\text{P}$ to form $[\text{tBu}_3\text{PH}][\text{SZO}_{300}]$ contrasts with NH_3 , a well-known probe for Brønsted sites, because NH_3 can also react with Lewis and strained sites on oxide surfaces.¹⁷

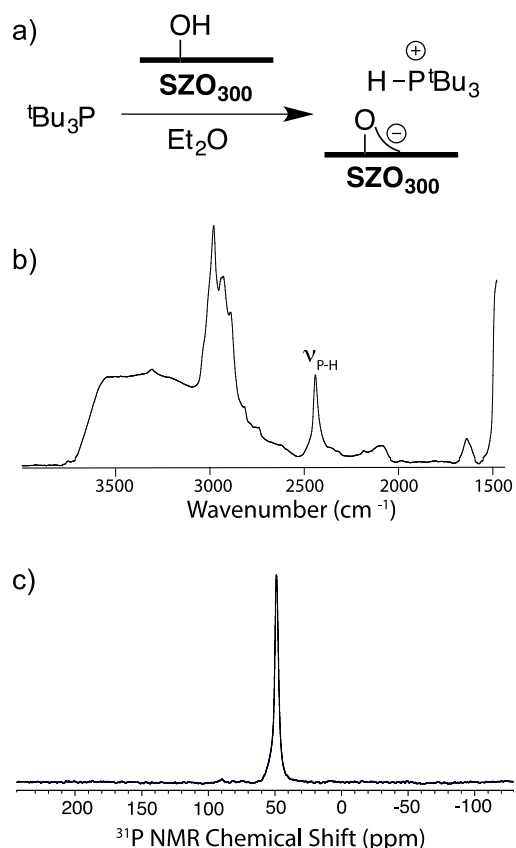
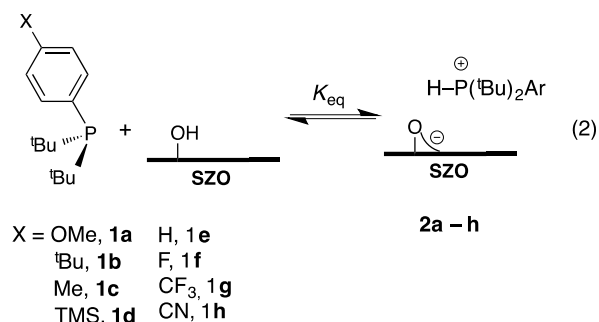


Figure 2. Reaction of $^t\text{Bu}_3\text{P}$ with **SZO**₃₀₀ to form $[\text{tBu}_3\text{PH}][\text{SZO}_{300}]$ (a); FTIR of $[\text{tBu}_3\text{PH}][\text{SZO}_{300}]$, the $\nu_{\text{P-H}}$ is labelled for clarity (b); $^{31}\text{P}\{^1\text{H}\}$ MAS NMR spectrum of this material (c).

$(^t\text{Bu})_2\text{ArP}$ (**1a – 1h**, eq 2), where the para position of the Ar group contains substituents that donate or withdraw electron density, were chosen to systematically evaluate how the electronics at phosphorous affects formation of



phosphonium sites on **SZO**₃₀₀. The reaction of (^tBu)₂ArP (**1a** – **1h**) with **SZO**₃₀₀ in MeCN slurry forms [(^tBu)₂ArPH][**SZO**₃₀₀] (**2a** – **2h**), eq 2. Table 1 contains key spectroscopic data for **2a** – **2h**. The ³¹P NMR chemical shifts of [**1H**][BF₄] are between 5 – 10 ppm downfield from **1a** – **1h** in CD₃CN solution, indicating that ³¹P NMR chemical shift can discriminate between free phosphine and [**1H**][BF₄]. The ³¹P{¹H} MAS spectra of **2a** – **2h** contain signals for the phosphonium at, or near, the values observed in [**1H**][BF₄]. Similar to the grafting of ^tBu₃P onto **SZO**₃₀₀, signals for oxidized products or (^tBu)₂ArP interacting with Lewis sites were not observed in ³¹P MAS spectra of **2a** – **2h**. In addition to the ³¹P MAS NMR spectra, the FTIR spectra of **2a** – **2h** contain ν_{P-H} stretches, decreasing from 2448 cm⁻¹ for **2a** to 2432 cm⁻¹ for **2h**.

Table 1. ³¹P NMR data for **1a** – **1h**, [**1H**][BF₄], and **2a** – **2h**.^a

(^t Bu) ₂ ArP	δ ³¹ P (ppm) ^b	δ ³¹ P (ppm) [1H][BF ₄] ^c	δ ³¹ P (ppm) 2a – 2h ^d	ν _{P-H} (cm ⁻¹) 2a – 2h
1a	36.4	46.8	43	2448
1b	41.8	46.7	46	2445
1c	37.6	47.6	46	2438
1d	39.9	44.7	48	2441
1e	38.9	48.0	49	2439
1f	37.1	46.8	48	2438
1g	38.4	47.2	49	2433
1h	39.0	47.4	46	2432

^a – referenced to 85 % H₃PO₄; ^b – CD₃CN solution; ^c – generated in CD₃CN solution (refer to the Supporting Information for details); ^d – 10 kHz MAS spinning speed.

Equilibrium binding studies were performed in anhydrous MeCN slurries at 25 °C under rigorously anaerobic conditions, experimental details are provided in the Supporting Information. A representative plot of the binding of **1a** to **SZO**₃₀₀ to form **2a** is shown in Figure 3. The data in Figure 3 relates to the equilibrium adsorption constant K_a , shown in eq 3, where [HO_x] are Brønsted sites on **SZO**₃₀₀ reported in mmol/g. K_a is extracted from fits of the data in Figure 3 to a single-site Langmuir isotherm, shown in eq 4, where [HO_x]₀ is the initial OH loading and θ is the surface coverage of the phosphine on **SZO**₃₀₀. K_a for the reaction of **SZO**₃₀₀ with **1a** to form **2a** is 7.4(4) × 10⁴ M⁻¹. The extracted binding constants from fits to eq 4 for other phosphines in this study, as well as p*K*_a values of [**1H**][BF₄] measured in CD₃CN solution,¹⁸ are given in Table 2. The prevailing trend of these data is that K_a decreases as p*K*_a of [**1H**] decreases. A Hammett plot from the data in Table 2 is linear with ρ = -0.14 (R² = 0.96, Figure S2), consistent with buildup of positive charge on phosphorus in the formation of **2a** – **2h**.

$$K_a = \frac{[2]}{[1][HO_x]} \quad (3)$$

$$\theta = \frac{K_a[1][HO_x]_0}{1 + K_a[1]} \quad (4)$$

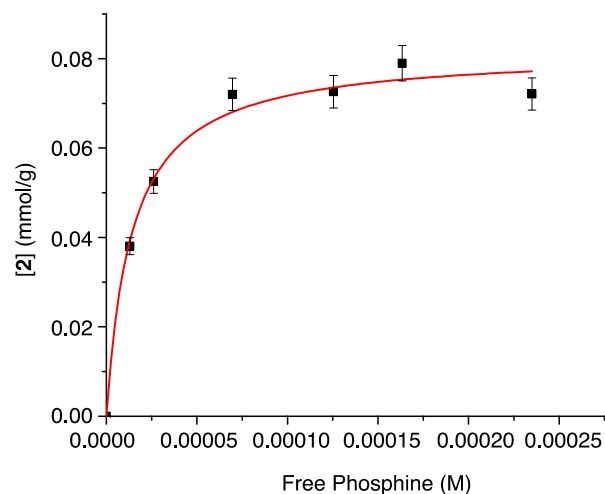


Figure 3. Langmuir isotherm of **1a** binding to **SZO**₃₀₀. The study was performed in triplicate using a phosphine stock solution of 0.3 mM, the error bars are standard deviations from these three binding studies.

Table 2. Binding constants for formation of **2** and p*K*_a of phosphoniums.

(^t Bu) ₂ ArP	K_a (×10 ⁴) ^a	p <i>K</i> _a [1H][BF ₄] ^b
1a	7.4(4)	16.4(1)
1b	5.5(3)	15.8(1)
1c	5.5(4)	15.7(2)
1d	4.7(1)	14.9(1)
1e	4.3(3)	14.7(1)
1f	3.0(2)	14.0(1)
1g	2.6(1)	12.9(1)
1h	1.9(4)	12.6(2)

^a – average of three binding studies in MeCN slurries, errors in parentheses are standard deviations from these data; ^b – determined in CD₃CN solution using methods described in ref 17, refer to the Supporting Information for details.

The data in Table 2 are inconsistent with Brønsted superacid behavior. Superacids are known to protonate MeCN to form [(MeCN)_xH][X] solvates.⁸ The p*K*_a of solvated protons in MeCN is 0,¹⁹ which should result in much stronger binding for bases whose conjugate acids have p*K*_a values as those in Table 2.

To test the strength of the acid sites on **SZO**₃₀₀ we contacted this material with Ph₃P. The pK_a of [Ph₃PH][BF₄] is 7.6 in MeCN, therefore Ph₃P should bind to **SZO**₃₀₀ weaker than (tBu)₂ArP described in Table 2. The reaction of **SZO**₃₀₀ with Ph₃P forms [Ph₃PH][**SZO**₃₀₀] (**4**) in MeCN. Similar to **2**, the ³¹P{¹H} MAS NMR chemical shift of **4** appears at a chemical shift close to those observed for solutions of [Ph₃PH][BF₄]. ³¹P{¹H} NMR studies of **SZO**₃₀₀ suspended in MeCN solutions containing PPh₃ show that K_a ~ 3 M⁻¹, indicating that PPh₃ binds much weaker than **1a** – **h**. This is consistent with the hypothesis that pK_a of [R₃PH] influences binding of phosphines to Brønsted sites on **SZO**₃₀₀.

The reaction of **SZO**₃₀₀ with (2-F-C₆H₄)Ph₂P in MeCN slurry, followed by successive washings with MeCN, does not contain a signals in the ³¹P{¹H} MAS NMR spectrum. Removal of MeCN of **SZO**₃₀₀ contacted with a solution of (2-F-C₆H₄)Ph₂P results in a ³¹P{¹H} MAS NMR spectrum containing a single signal at -8 ppm, the chemical shift of (2-F-C₆H₄)Ph₂P in CD₃CN solution is -8.3 ppm. These data indicate that (2-F-C₆H₄)Ph₂P does not react with Brønsted sites on **SZO**₃₀₀. [(2-F-C₆H₄)Ph₂PH][BF₄] has a pK_a of 6.11 in MeCN.²⁰ This result establishes that the -OH sites on **SZO**₃₀₀ do not protonate bases whose conjugate acid has a pK_a of 6.11 or below. This assertion is supported by the reaction of **SZO**₃₀₀ with an acetonitrile solution of *p*-nitroaniline (pK_a(anilinium) = 6.22 in CH₃CN),²¹ a common Hammett indicator. Contacting **SZO**₃₀₀ with bright yellow MeCN solutions of *p*-nitroaniline results in a bright yellow solution and a white solid after successive washing with MeCN (Figure S4). This result indicates that *p*-nitroaniline is not protonated by the acid sites on **SZO**₃₀₀. Consistent with this observation, the FTIR spectrum of **SZO**₃₀₀ contacted with *p*-nitroaniline lacks the ν_{NH} stretch of *p*-nitroanilinium (Figure S5).

The reaction of phosphines with **SZO**₃₀₀ produces [R₃PH][**SZO**₃₀₀] without formation of byproducts that would arise from side reactions on this material. The clean formation of [R₃PH][**SZO**₃₀₀] allowed an evaluation of how pK_a in [R₃PH] is related to surface binding. These studies clearly show that the -OH sites on **SZO**₃₀₀ cannot be superacidic. If these sites were superacidic, **SZO**₃₀₀ would certainly protonate (2-F-C₆H₄)Ph₂P, let alone less basic phosphines. The weak acidity of the Brønsted sites on **SZO**₃₀₀ suggest they are probably not involved in alkane isomerization reactions.^{9,12} However, pyrosulfate formed during the material synthesis is

implicated in reactions with C-H bonds,¹² and can also play a role in organometallic grafting reactions.^{5a} Since the quantity of pyrosulfate is related to thermal activation temperatures appropriate thermal treatment of these materials prior to grafting and/or catalysis requires special attention.

ASSOCIATED CONTENT

Supporting Information.

The Supporting Information is available free of charge on the ACS Publications website:

Experimental details, solid-state NMR spectra, pK_a determinations, Langmuir titration data (PDF)

AUTHOR INFORMATION

Corresponding Author

*matthew.conley@ucr.edu

Funding Sources

No competing financial interests have been declared.

ORCID

Matthew P. Conley: 0000-0001-8593-5814

ACKNOWLEDGMENT

M. P. C. is a member of the UCR Center for Catalysis. This work was supported by the National Science Foundation (CHE-1800561). Solid-state NMR measurements were recorded on an instrument supported by the National Science Foundation (CHE-1626673).

REFERENCES

- (1) a) Copéret, C.; Chabanas, M.; Petroff Saint-Arroman, R.; Basset, J.-M. Homogeneous and Heterogeneous Catalysis: Bridging the Gap through Surface Organometallic Chemistry. *Angew. Chem., Int. Ed.* **2003**, *42*, 156-181; b) Marks, T. J. Surface-bound metal hydrocarbyls. Organometallic connections between heterogeneous and homogeneous catalysis. *Acc. Chem. Res.* **1992**, *25*, 57-65; c) Wegener, S. L.; Marks, T. J.; Stair, P. C. Design Strategies for the Molecular Level Synthesis of Supported Catalysts. *Acc. Chem. Res.* **2011**, *45*, 206-214; d) Copéret, C.; Comas-Vives, A.; Conley, M. P.; Estes, D. P.; Fedorov, A.; Mougél, V.; Nagae, H.; Núñez-Zarur, F.;

- Zhizhko, P. A. Surface Organometallic and Coordination Chemistry toward Single-Site Heterogeneous Catalysts: Strategies, Methods, Structures, and Activities. *Chem. Rev.* **2016**, *116*, 323-421; e) Guzman, J.; Gates, B. C. Supported molecular catalysts: metal complexes and clusters on oxides and zeolites. *Dalton Trans.* **2003**, *17*, 3303-3318; f) Copéret, C.; Allouche, F.; Chang, K. W.; Conley, M.; Delley, M. F.; Fedorov, A.; Moroz, I.; Mougél, V.; Pucino, M.; Searles, K.; Yamamoto, K.; Zhizhko, P. Bridging the Gap between Industrial and Well-Defined Supported Catalysts. *Angew. Chem., Int. Ed.* **2018**, *57*, 6398-6440; g) Basset, J.-M.; Coperet, C.; Soulivong, D.; Taoufik, M.; Cazat, J. T. Metathesis of Alkanes and Related Reactions. *Acc. Chem. Res.* **2009**, *43*, 323-334; h) Basset, J. M.; Choplin, A., Surface organometallic chemistry: A new approach to heterogeneous Catalysis? *J. Mol. Catal.* **1983**, *21*, 95-108; i) Ballard, D. G. H., Pi and Sigma Transition Metal Carbon Compounds as Catalysts for the Polymerization of Vinyl Monomers and Olefins. In *Advances in Catalysis*, D.D. Eley, H. P.; Paul, B. W., Eds. Academic Press: 1973; Vol. Volume 23, pp 263-325; j) Yermakov, Y. I., Anchored Complexes in Fundamental Catalytic Research. In *Studies in Surface Science and Catalysis*, Seivama, T.; Tanabe, K., Eds. Elsevier: 1981; Vol. Volume 7, Part A, pp 57-76.
- (2) Jezequel, M.; Dufaud, V.; Ruiz-Garcia, M. J.; Carrillo-Hermosilla, F.; Neugebauer, U.; Niccolai, G. P.; Lefebvre, F.; Bayard, F.; Corker, J.; Fiddy, S.; Evans, J.; Broyer, J.-P.; Malinge, J.; Basset, J.-M. Supported Metallocene Catalysts by Surface Organometallic Chemistry. Synthesis, Characterization, and Reactivity in Ethylene Polymerization of Oxide-Supported Mono- and Biscyclopentadienyl Zirconium Alkyl Complexes: Establishment of Structure/Reactivity Relationships. *J. Am. Chem. Soc.* **2001**, *123*, 3520-3540.
- (3) a) Review: Stalzer, M.; Delferro, M.; Marks, T. Supported Single-Site Organometallic Catalysts for the Synthesis of High-Performance Polyolefins. *Catal. Lett.* **2015**, *145*, 3-14; b) For late transition metal sites for olefin polymerization see: Culver, D. B.; Tafazolian, H.; Conley, M. P. A Bulky Pd(II) α -Diimine Catalyst Supported on Sulfated Zirconia for the Polymerization of Ethylene and Copolymerization of Ethylene and Methyl Acrylate. *Organometallics* **2018**, *37*, 1001-1006; c) Tafazolian, H.; Culver, D. B.; Conley, M. P. A Well-Defined Ni(II) α -Diimine Catalyst Supported on Sulfated Zirconia for Polymerization Catalysis. *Organometallics* **2017**, *36*, 2385-2388.
- (4) a) Marie, S. M.; P., N. C.; Alak, B.; Alessandro, M.; Massimiliano, D.; J., M. T. Single-Face/All-cis Arene Hydrogenation by a Supported Single-Site d^0 Organozirconium Catalyst. *Angew. Chem., Int. Ed.* **2016**, *55*, 5263-5267; b) Gu, W.; Stalzer, M. M.; Nicholas, C. P.; Bhattacharyya, A.; Motta, A.; Gallagher, J. R.; Zhang, G.; Miller, J. T.; Kobayashi, T.; Pruski, M.; Delferro, M.; Marks, T. J. Benzene Selectivity in Competitive Arene Hydrogenation: Effects of Single-Site Catalyst***Acidic Oxide Surface Binding Geometry. *J. Am. Chem. Soc.* **2015**, *137*, 6770-6780; c) Williams, L. A.; Guo, N.; Motta, A.; Delferro, M.; Fragala, I. L.; Miller, J. T.; Marks, T. J. Surface structural-chemical characterization of a single-site d^0 heterogeneous arene hydrogenation catalyst having 100% active sites. *Proc. Nat. Acad. Sci. USA* **2013**, *110*, 413-418.
- (5) a) Klet, R. C.; Kaphan, D. M.; Liu, C.; Yang, C.; Kropf, A. J.; Perras, F. A.; Pruski, M.; Hock, A. S.; Delferro, M. Evidence for Redox Mechanisms in Organometallic Chemisorption and Reactivity on Sulfated Metal Oxides. *J. Am. Chem. Soc.* **2018**, *140*, 6308-6316; b) Kaphan, D. M.; Klet, R. C.; Perras, F. A.; Pruski, M.; Yang, C.; Kropf, A. J.; Delferro, M. Surface Organometallic Chemistry of Supported Iridium(III) as a Probe for Organotransition Metal-Support Interactions in C-H Activation. *ACS Catal.* **2018**, *8*, 5363-5373.
- (6) Culver, D. B.; Conley, M. P. Activation of C-F Bonds by Electrophilic Organosilicon Sites Supported on Sulfated Zirconia. *Angew. Chem., Int. Ed.* **2018**, *57*, 14902-14905.
- (7) a) Hino, M.; Kobayashi, S.; Arata, K. Solid catalyst treated with anion. 2. Reactions of butane and isobutane catalyzed by zirconium oxide treated with sulfate ion. Solid superacid catalyst. *J. Am. Chem. Soc.* **1979**, *101*, 6439-6441; b) Hino, M.; Arata, K. Synthesis of solid superacid catalyst with acid strength of $H_0 \leq -16.04$. *Chem. Commun.* **1980**, 851-852.
- (8) Olah, G. A.; Prakash, G. K. S.; Sommer, J.; Molnar, A.: *Superacid Chemistry*, John Wiley & sons, 2009.
- (9) Tabora, J. E.; Davis, R. J. On the Superacidity of Sulfated Zirconia Catalysts for Low-Temperature

- 1
2
3
4
5
6
7
8
9
10
11
12
13
14
15
16
17
18
19
20
21
22
23
24
25
26
27
28
29
30
31
32
33
34
35
36
37
38
39
40
41
42
43
44
45
46
47
48
49
50
51
52
53
54
55
56
57
58
59
60
- Isomerization of Butane. *J. Am. Chem. Soc.* **1996**, *118*, 12240-12241.
- (10) Drago, R. S.; Kob, N. Acidity and Reactivity of Sulfated Zirconia and Metal-Doped Sulfated Zirconia. *J. Phys. Chem. B* **1997**, *101*, 3360-3364.
- (11) Haw, J. F.; Zhang, J.; Shimizu, K.; Venkatraman, T. N.; Luigi, D.-P.; Song, W.; Barich, D. H.; Nicholas, J. B. NMR and Theoretical Study of Acidity Probes on Sulfated Zirconia Catalysts. *J. Am. Chem. Soc.* **2000**, *122*, 12561-12570.
- (12) a) Haase, F.; Sauer, J. The Surface Structure of Sulfated Zirconia: Periodic ab Initio Study of Sulfuric Acid Adsorbed on ZrO₂(101) and ZrO₂(001). *J. Am. Chem. Soc.* **1998**, *120*, 13503-13512; b) Li, X.; Nagaoka, K.; Simon, L. J.; Olindo, R.; Lercher, J. A.; Hofmann, A.; Sauer, J. Oxidative Activation of n-Butane on Sulfated Zirconia. *J. Am. Chem. Soc.* **2005**, *127*, 16159-16166.
- (13) Farneth, W. E.; Gorte, R. J. Methods for Characterizing Zeolite Acidity. *Chem. Rev.* **1995**, *95*, 615-635.
- (14) Stoyanov, E. S.; Kim, K.-C.; Reed, C. A. An Infrared ν_{NH} Scale for Weakly Basic Anions. Implications for Single-Molecule Acidity and Superacidity. *J. Am. Chem. Soc.* **2006**, *128*, 8500-8508.
- (15) a) Osegovic, J. P.; Drago, R. S. Measurement of the Global Acidity of Solid Acids by ³¹P MAS NMR of Chemisorbed Triethylphosphine Oxide. *J. Phys. Chem. B* **1999**, *104*, 147-154; b) Farcasiu, D.; Ghenciu, A. Acidity functions from carbon-13 NMR. *J. Am. Chem. Soc.* **1993**, *115*, 10901-10908.
- (16) Haav, K.; Saame, J.; Kütt, A.; Leito, I. Basicity of Phosphanes and Diphosphanes in Acetonitrile. *Eur. J. Org. Chem.* **2012**, *2012*, 2167-2172.
- (17) a) Asefa, T.; Kruk, M.; Coombs, N.; Grondey, H.; MacLachlan, M. J.; Jaroniec, M.; Ozin, G. A., Novel Route to Periodic Mesoporous Aminosilicas, PMAs: Ammonolysis of Periodic Mesoporous Organosilicas. *J. Am. Chem. Soc.* **2003**, *125*, 11662-11673; b) Hamzaoui, B.; Bendjeriou-Sedjerari, A.; Pump, E.; Abou-Hamad, E.; Sougrat, R.; Gurinov, A.; Huang, K.-W.; Gajan, D.; Lesage, A.; Emsley, L.; Basset, J.-M., Atomic-level organization of vicinal acid-base pairs through the chemisorption of aniline and derivatives onto mesoporous SBA15. *Chem. Sci.* **2016**, *7*, 6099-6105; c) Bendjeriou-Sedjerari, A.; Pelletier, J. D. A.; Abou-hamad, E.; Emsley, L.; Basset, J.-M., A well-defined mesoporous amine silica surface via a selective treatment of SBA-15 with ammonia. *Chem. Commun.* **2012**, *48*, 3067-3069.
- (18) Abdur-Rashid, K.; Fong, T. P.; Greaves, B.; Gusev, D. G.; Hinman, J. G.; Landau, S. E.; Lough, A. J.; Morris, R. H. An Acidity Scale for Phosphorus-Containing Compounds Including Metal Hydrides and Dihydrogen Complexes in THF: Toward the Unification of Acidity Scales. *J. Am. Chem. Soc.* **2000**, *122*, 9155-9171.
- (19) Morris, R. H. Brønsted-Lowry Acid Strength of Metal Hydride and Dihydrogen Complexes. *Chem. Rev.* **2016**, *116*, 8588-8654.
- (20) Greb, L.; Tussing, S.; Schirmer, B.; Oña-Burgos, P.; Kaupmees, K.; Lökov, M.; Leito, I.; Grimme, S.; Paradies, J. Electronic effects of triarylphosphines in metal-free hydrogen activation: a kinetic and computational study. *Chem. Sci.* **2013**, *4*, 2788-2796.
- (21) Kaljurand, I.; Kütt, A.; Sooväli, L.; Rodima, T.; Mäemets, V.; Leito, I.; Koppel, I. A. Extension of the Self-Consistent Spectrophotometric Basicity Scale in Acetonitrile to a Full Span of 28 pK_a Units: Unification of Different Basicity Scales. *J. Org. Chem.* **2005**, *70*, 1019-1028.

